Electronic structure and magnetic ordering of the semiconducting chromium trihalides $CrCl_3$, $CrBr_3$, and CrI_3

J. Phys.: Condens. Matter **23** (2011) 116003 (8pp) doi:10.1088/0953-8984/23/11/116003

Electronic structure and magnetic ordering of the semiconducting chromium trihalides $CrCl_3$, $CrBr_3$, and CrI_3

H Wang[1], V Eyert[2] and U Schwingenschlögl[1]

[1] PSE Division, KAUST, Thuwal 23955-6900, Saudi Arabia
[2] Centre for Electronic Correlations and Magnetism, University of Augsburg, D-86135 Augsburg, Germany

E-mail: udo.schwingenschlogl@kaust.edu.sa

Received 16 November 2010, in final form 29 December 2010
Published 1 March 2011
Online at stacks.iop.org/JPhysCM/23/116003

Abstract

We present results from an electronic structure investigation of the chromium halides $CrCl_3$, $CrBr_3$, and CrI_3, as obtained by the linearized augmented plane wave method of density functional theory. Our interest focuses on the chloride. While all three halides display strong ferromagnetic coupling within the halide–Cr–halide triple layers, our emphasis is on differences in the interlayer magnetic coupling. In agreement with experimental results, our calculations indicate ferromagnetic ordering for $CrBr_3$ as well as CrI_3. The antiferromagnetic state of $CrCl_3$ can be reproduced by introducing an on-site electron–electron repulsion. However, we observe that the ground state depends critically on the specific approach used. Our results show that a low temperature structural phase transition from monoclinic to trigonal is energetically favourable for $CrCl_3$.

(Some figures in this article are in colour only in the electronic version)

1. Introduction

Despite extensive experimental and theoretical investigations, understanding of the magnetic properties of the non-metallic 3d transition metal halides $CrCl_3$, $CrBr_3$, and CrI_3 is still far from complete. All three compounds exhibit a strong intralayer ferromagnetic coupling, as expected from the Goodenough–Kanamori–Anderson rules [1–3]. In particular, $CrBr_3$ was the first ferromagnetic semiconductor, found by Tsubokawa in 1960 [4]. While the interlayer coupling is ferromagnetic for $CrBr_3$ and CrI_3, it is antiferromagnetic for $CrCl_3$, with critical temperatures of $T_N^{Cl} = 16.8$ K, $T_C^{Br} = 32.5$ K, and $T_C^{I} = 68$ K [5]. For $CrCl_3$, the same critical temperature has been already reported by Starr *et al* together with a paramagnetic Curie temperature of 27 K [6]. Whereas the spins of the chloride lie in the basal plane of the crystal structure, the easy spin axis of the bromide and the iodide is oriented perpendicular to the basal plane.

Structurally, the three chromium halides are closely related layered systems. For this reason, the differences in magnetic couplings are surprising. As a consequence, the chromium halides and the mechanisms driving the exchange coupling have been the subject of interest for many years. In our paper we present the results of band structure calculations in order to contribute to a deeper understanding of the compounds. We focus on $CrCl_3$.

Magnetic susceptibility measurements of de Jongh and Miedema [7] revealed strong ferromagnetic intralayer coupling for all three compounds with coupling constants of $J = -4.1$ meV for $CrCl_3$, $J = -6.4$ meV for $CrBr_3$ and $J = -10.5$ meV for CrI_3. Hence, the magnetic coupling becomes stronger on going from the chloride to the iodide. According to spin wave dispersion as inferred from inelastic neutron scattering measurements for $CrBr_3$ by Samuelsen *et al* [8] the intralayer next nearest neighbour coupling amounts to $J = -7.6$ meV. High-frequency susceptibility measurements for single-crystal $CrBr_3$ samples confirmed a transition temperature of almost 33 K, where a description in terms of a 3D Heisenberg ferromagnet becomes adequate [9]. Spin wave analysis yields isotropic ferromagnetic intralayer exchange constants of 5.25 K for $CrCl_3$ and of 8.25 K for $CrBr_3$, whereas the interlayer coupling amounts to -0.018 K and 0.497 K, respectively [10, 11]. As a consequence, the magnetic coupling in the chloride is much more 2D like as

compared to the bromide. Thus, $CrCl_3$ is on the verge of an effective magnetic decoupling of the planes.

According to photoelectron spectroscopy results, see [12–14] and [15], for $CrCl_3$ and $CrBr_3$ the Cr 3d states are located near the Fermi level, well above the halide 3p/4p/5p states. In general, this has been confirmed by self-consistent band structure calculations for $CrCl_3$ and $CrBr_3$ by Antoci and Mihich [16], who used the intersecting-spheres model. Because spin degeneracy was enforced in these calculations, a metallic behaviour was observed. This lead Pollini and co-workers to the conclusion that strong electronic correlations are responsible for the semiconducting behaviour and, hence, must be included in the calculations. Transition energies calculated by Shinagawa *et al* [17] within a cluster model compare well to experimental findings.

Feldkemper and Weber [18] have calculated the magnetic coupling constants in the framework of a multiband Hubbard model. Using a Rayleigh–Schrödinger perturbation expansion to map the original model onto an effective Heisenberg Hamiltonian they have been able to describe the superexchange coupling between the magnetic sites. Their calculations included interaction paths via arbitrarily many ligands and, hence, exceeded the predictions of the Goodenough–Kanamori–Anderson rules. According to their results, the antiferromagnetic interlayer coupling is overcompensated by ferromagnetic coupling in all three halides in their trigonal structures. In contrast, the correct antiferromagnetic coupling of $CrCl_3$ could only be reproduced for an unphysical parameter set. For this reason, the authors concluded that the crystal structure of $CrCl_3$ does not have $R\bar{3}$ symmetry, as previously claimed by Morosin and Narath [19]. As a matter of fact, state-of-the-art electronic structure calculations, which could help to resolve this contradiction, have not been reported so far.

2. Structural considerations and technical details

At low temperatures the chromium trihalides crystallize in the trigonal BiI_3 structure with space group $R\bar{3}$ [8, 19, 20]. As we show in figure 1, the unit cell contains two formula units. The Cr atoms occupy crystallographically equivalent positions, as do the halide atoms. The structure consists of halide–Cr–halide triple layers, which are stacked along the hexagonal c-axis. Adjacent triple layers are bonded by weak van der Waals forces. While the central Cr atoms of each sandwich form a honeycomb lattice, both these atoms and the vacancies in the centre of the hexagons are surrounded by edge-sharing octahedra of halide atoms. The octahedral coordination of Cr by six Cl atoms resembles the transition metal filled oxygen octahedra known from transition metal oxides [21, 22]. Neighbouring triple layers are shifted perpendicular to the c-axis such that each fourth reproduces the atomic arrangement of the initial triple layer. The halide layers are formed by the triangular faces of the halide octahedra perpendicular to the c-axis. As a consequence, the halide sublattice may approximately be described in terms of a hexagonal close-packed arrangement. This means halide layers alternate along the c-axis with respect to the stacking sequence A–B. Thus, the full stacking sequence is A–Cr–B $\cdots$ A–Cr–B $\cdots$ A–Cr–B.

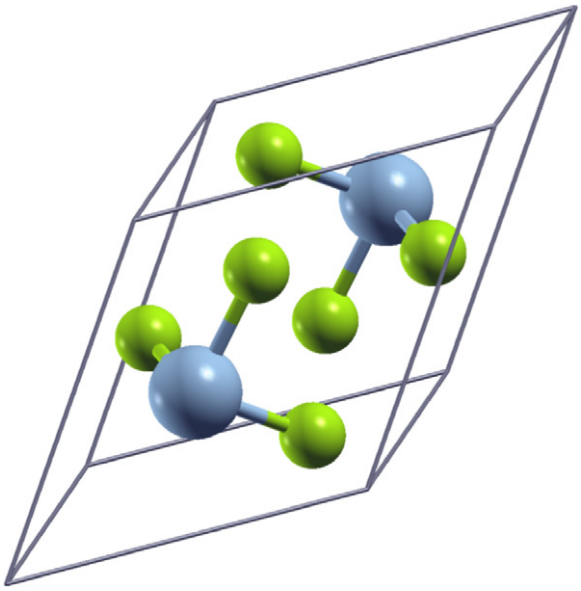

Figure 1. Trigonal unit cell of $Cr(Cl/Br/I)_3$ with Cr atoms shown as large grey spheres and Cl/Br/I atoms as small green spheres.

The crystal structure of $CrCl_3$ has been investigated by Morosin and Narath [19], who have observed a phase transition from the monoclinic $C2/m$ to the trigonal $R\bar{3}$ symmetry near 240 K. However, this transition has not been confirmed by other groups. The monoclinic configuration of $CrCl_3$ is based on almost the same atomic arrangement. Only the stacking sequence of the halide layers is different, since the halide sublattice here has a face-centred cubic closed-packed arrangement with the stacking sequence A–B–C. As a consequence, the stacking of the complete structure is given by A–Cr–B $\cdots$ C–Cr–A $\cdots$ B–Cr–C. Note that for both the trigonal and the monoclinic structure the separation between neighbouring halide planes is almost 20% smaller if it is filled by a chromium layer, as compared to adjacent halide planes. Since the calculations of Feldkemper and Weber [18] cast doubts on the $R\bar{3}$ symmetry of the chloride, we will address electronic band structures for the proposed trigonal and monoclinic structures and compare the calculated magnetic moments to experimental findings.

Morosin and Narath [19] found a volume change of less than 1% at the $C2/m$ to $R\bar{3}$ phase transition. Nuclear quadrupole resonance studies of twinned powder samples result in two resonances at room temperature but only a single resonance at low temperature. Consequently, the symmetry of the crystal increases on going from the high into the low temperature phase. The same first order $C2/m$ to $R\bar{3}$ phase transition, coming along with a lateral shift of the halide–Cr–halide triple layers, is found for $CrBr_3$ near 420 K. However, measurements of the phase transition of $CrCl_3$ seem to be strongly affected by crystal imperfections, since large fractions of the samples remain monoclinic at low temperature. A twinning of the crystals along the hexagonal c-axis cannot be avoided.

In table 1 we report the experimental Cr–halide bond lengths for the different compounds. Starting from these values, we have fully optimized the lattice constants and atomic

Table 1. Distances between the octahedral Cr and the corresponding halide sites for three chromium halides (in Å).

Compound	Symmetry	Cr–Halide bond length
$CrCl_3$	Trigonal	2.364 A(3×) 2.328(3×)
$CrCl_3$	Monoclinic	2.348 A(2×) 2.342(2×) 2.340(2×)
$CrBr_3$	Trigonal	2.517 A(3×) 2.456(3×)
CrI_3	Trigonal	2.800 A(6×)

Table 2. Volume increase (ΔV) between the best optimized solution and experimental structure.

Compound	Method	ΔV NM (%)	ΔV FM (%)	ΔV AF (%)
$CrCl_3$ trigonal	GGA	0	3.5	3
	GGA + AMF	0	5	4
	GGA + SIC	2	8	7
	GGA + HMF	1	6	6
$CrCl_3$ monoclinic	GGA	1	3	2
	GGA + AMF	—	4	4
	GGA + SIC	—	7	7
	GGA + HMF	—	5	5
$CrBr_3$ trigonal	GGA	0	5	5
CrI_3 trigonal	GGA	−5	0	0

coordinates for various methods. The results of the obtained volume change are summarized in table 2 and the optimized bond lengths are given in table 3.

We use the linearized augmented plane wave approach of the WIEN2k package [23], which is suitable for treating magnetic systems with high accuracy [24]. To ensure efficiency and accuracy of the calculations, the choice of the k-points and plane wave cutoff, $RK_{max} = 8.5$, has been optimized. Converged results have been obtained for the $R\bar{3}$ symmetry for 226 (NM, FM) and 666 (AF) k-points in the irreducible wedge of the Brillouin zone, generated from a $11 \times 11 \times 11$ k-mesh. For the $C2/m$ symmetry 324 k-points have been generated from a $14 \times 6 \times 14$ k-mesh. We use muffin-tin radii (in atomic units) of 2.25 (Cr) and 1.99 (Cl) for the chloride, 2.37 (Cr) and 2.10 (Br) for the bromide, as well as 2.50 (Cr) and 2.50 (I) for the iodide. Besides the generalized gradient approximation (GGA), the following three GGA + U approaches have been employed: the around mean-field method (GGA + AMF) [25], the Hubbard mean field method (GGA + HMF) [26], and the self-interaction correction method (GGA + SIC) [27]. They allow us to take into account the effects of the on-site Coulomb repulsion U, which is known to be relevant for $CrCl_3$. A value of $U = 0.3$ Ryd is employed. All calculations have been carried out non-magnetically (NM) as well as assuming ferromagnetic (FM) and antiferromagnetic (AF) spin order. By means of the NM calculations we address general issues such as the crystal field splitting and the hybridization. Afterwards, we will analyse the magnetic coupling via spin polarized results.

3. Results and discussion

All the results discussed in the following are based on fully optimized crystal structures. This fact allows us to determine the lowest energy structures of the chromium halides for the different spin configurations and approximation methods. All three investigated compounds show in the NM density of states (DOS) three groups of bands in the vicinity of the Fermi energy, see figure 2 for $CrCl_3$, due to the octahedral coordination of the Cr sites. Figure 2 displays a slightly metallic state which, however, is on the verge of an insulator. The first of the mentioned groups extends from −6.5 to −2 eV, originating from the halide 3p states. The second group is found at the Fermi level, tracing back to the Cr 3d t_{2g} states. Finally, the third group consists of a sharp peak near 2 eV, comprising the Cr 3d e_g states. These findings are consistent with results from photoelectron spectroscopy [12–15] and with the electronic structure calculations of Antoci and Mihich [16].

Applying the GGA approach, figure 2 also compares the NM DOS (top) to corresponding results for the FM configuration (middle), where ferromagnetic coupling of the Cr atoms is assumed, and for the AF configuration (bottom), where antiferromagnetic coupling of the two Cr atoms in the unit cell (which belong to two neighbouring triple layers) is assumed. Comparing the NM to the spin polarized results allows us to identify the effects of the magnetic ordering on the band structure. In the AF case, it is found that the states shift to higher energy and peaks sharpen as compared to the FM case. We observe that the AF configuration has a higher total energy than the FM configuration, compare the summary of energies in table 1. The FM DOS reveals a strong spin splitting of about 3 eV and an insulating energy gap of 1.63 eV. Spin majority and minority bands are coloured black and red (grey) in the

Table 3. Distances between the octahedral Cr and the corresponding halide sites in the best optimized structure (in Å).

Compound	Method	Bond length NM	Bond length FM	Bond length AF
$CrCl_3$ trigonal	GGA	2.293(3×) 2.291(3×)	2.338(3×) 2.337(3×)	2.342(3×) 2.337(3×)
	GGA + AMF	2.333(3×) 2.325(3×)	2.349(3×) 2.348(3×)	2.346(3×) 2.344(3×)
	GGA + SIC	2.338(3×) 2.337(3×)	2.371(3×) 2.370(3×)	2.370(3×) 2.368(3×)
	GGA + HMF	2.334(3×) 2.328(3×)	2.361(6×)	2.367(3×) 2.360(3×)
$CrCl_3$ monoclinic	GGA	2.295(4×) 2.292(2×)	2.340(2×) 2.338(2×) 2.337(2×)	2.337(2×) 2.334(2×) 2.333(2×)
	GGA + AMF	—	2.353(2×) 2.348(2×) 2.346(2×)	2.353(2×) 2.348(2×) 2.346(2×)
	GGA + SIC	—	2.372(2×) 2.370(4×)	2.373(4×) 2.371(2×)
	GGA + HMF	—	2.364(2×) 2.360(2×) 2.358(2×)	2.363(2×) 2.360(2×) 2.358(2×)
$CrBr_3$ trigonal	GGA	2.445(6×)	2.496(6×)	2.496(1×) 2.495(2×) 2.492(2×) 2.491(1×)
CrI_3 trigonal	GGA	2.650(3×) 2.649(3×)	2.705(3×) 2.704(3×)	2.704(3×) 2.703(1×) 2.701(2×)

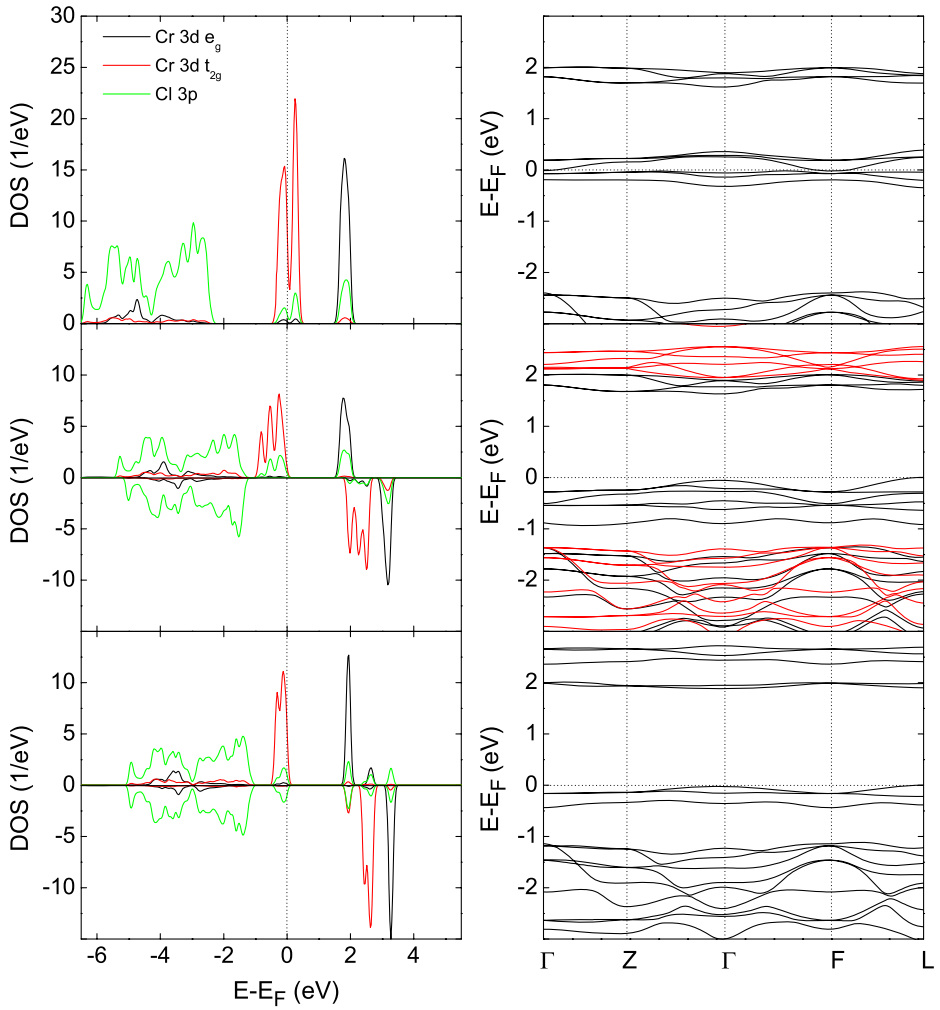

Figure 2. Partial DOS and band structure of trigonal $CrCl_3$ obtained from GGA calculations for the NM (top), FM (middle), and AF (bottom) configurations.

spin polarized band structure on the right-hand side of figure 2, respectively.

Hybridization of chromium and chloride states results in Cl 3p admixtures in the energy range dominated by the Cr states, which are stronger for σ-type bonding e_g states. Octahedral coordination of the transition metal atoms leads to an almost perfect energetical separation between the t_{2g} and e_g groups of bands. Small contributions of the t_{2g} states in the e_g energy range and vice versa are a consequence of small distortions of the Cl octahedra due to the fact that Cr-filled and empty halide layers alternate along the c-axis.

In figure 3 we show the DOS of trigonal $CrCl_3$ obtained by the GGA + AMF (left) and GGA + HMF (right) methods. Here and in the following we do not provide results for the GGA + SIC method, because those turn out to be very similar to the GGA + HMF results and therefore do not provide any new insights. In the NM case, the GGA + AMF and GGA + HMF DOSs are almost identical. There are four groups of bands occupying the energy ranges from −5.6 to −1.2 eV, −0.8 to 0.2 eV, 1.0 to 1.8 eV, and 2.4 eV to 3.1 eV. For both spin polarized calculations, the spin majority and minority peaks above Fermi energy show the opposite energetical order for the GGA + AMF and GGA + HMF methods. Therefore, only the GGA + AMF method reproduces the experimental result that the system favours AF coupling rather than FM coupling, see table 4. In addition, while usually we find the band gap in the AF case to be larger than in the FM case, this is different for the GGA + AMF results, for both the trigonal and monoclinic symmetry.

Using the same representation as figures 2 and 4 gives the band structures and DOSs obtained for the monoclinic crystal structure of $CrCl_3$. In contrast to the trigonal case, our GGA calculations now indicate that the total energies of the FM and AF configurations almost degenerate under the structure optimization, see table 1. The DOS looks rather similar to that obtained for the trigonal structure, except that the Cr 3d t_{2g} dominated bands in the AF case show more dispersion as well as a smaller separation from each other. Again, the spin polarized results reveal a strong spin splitting of about 3 eV and insulating energy gaps of 1.54 eV (FM) and 1.75 eV (AF). Concerning the Cr–Cl hybridization and the splitting due to the octahedral crystal field no differences are found as compared to the trigonal structure.

Figure 5 deals with GGA + AMF and GGA + HMF results for the monoclinic structure, analogous to figure 3. However, since the NM configuration obviously is very

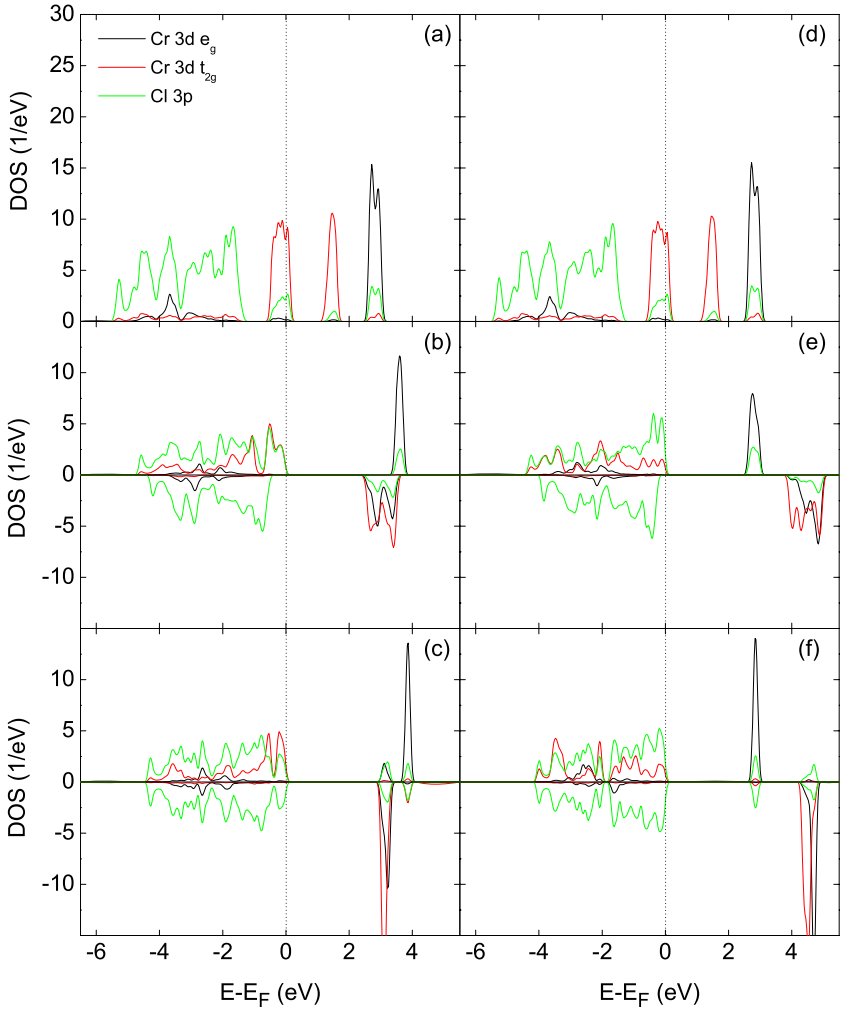

Figure 3. Partial DOS of trigonal $CrCl_3$ obtained from GGA + AMF (left) and GGA + HMF (right) calculations for the NM (top), FM (middle), and AF (bottom) configurations.

Table 4. Energy differences between the NM and FM/AF solutions (eV per 2 Cr), Cr moment (μ_B) and energy gap (eV) for the chromium halides. For the chloride two different crystal structures are considered.

Compound	Method	Optimization	$E_{FM} - E_{NM}$	Moment FM	Gap FM	$E_{AF} - E_{NM}$	Moment AF	Gap AF
$CrCl_3$ trigonal	GGA	No	−3.05	2.78	1.65	−3.03	2.72	1.83
		Yes	−2.90	2.77	1.63	−2.88	2.71	1.86
	GGA + AMF	No	−3.49	2.51	3.41	−3.51	2.47	2.96
		Yes	−3.53	2.51	3.43	−3.54	2.47	2.98
	GGA + SIC	No	−6.46	2.93	2.73	−6.43	2.90	2.89
		Yes	−6.54	2.95	2.69	−6.50	2.92	2.86
	GGA + HMF	No	−6.43	2.95	2.63	−6.39	2.91	2.80
		Yes	−6.49	2.96	2.62	−6.45	2.93	2.78
$CrCl_3$ monoclinic	GGA	No	−3.03	2.78	1.56	−3.04	2.77	1.78
		Yes	−2.90	2.77	1.54	−2.90	2.77	1.75
	GGA + AMF	No	—	2.51	3.39	—	2.51	2.56
		Yes	—	2.51	3.40	—	2.51	2.56
	GGA + SIC	No	—	2.93	2.68	—	2.93	2.92
		Yes	—	2.96	2.58	—	2.96	2.80
	GGA + HMF	No	—	2.94	2.57	—	2.94	2.82
		Yes	—	2.96	2.51	—	2.96	2.74
$CrBr_3$ trigonal	GGA	No	−3.04	2.87	1.36	−3.01	2.81	1.62
		Yes	−2.97	2.84	1.37	−2.93	2.82	1.62
CrI_3 trigonal	GGA	No	−3.33	3.12	0.74	−3.28	3.07	0.90
		Yes	−2.89	3.00	1.08	−2.84	2.93	1.30

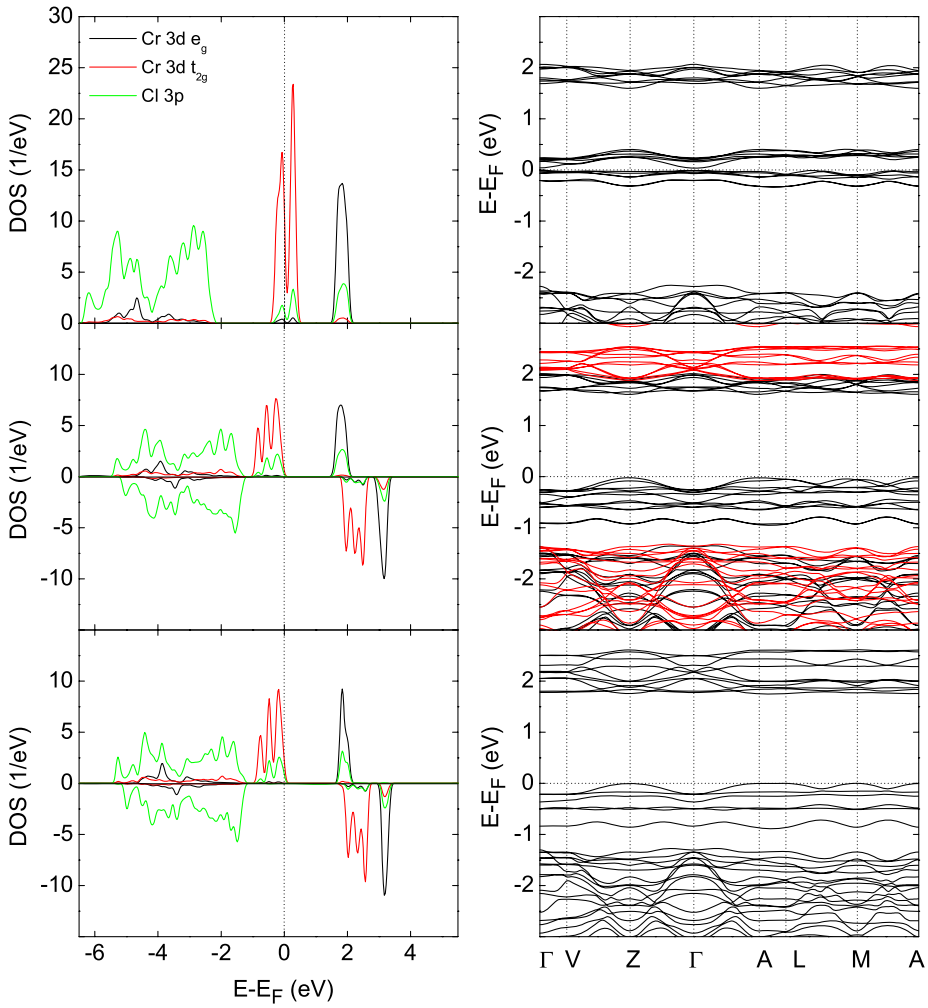

Figure 4. Partial DOS and band structure of monoclinic $CrCl_3$ obtained from GGA calculations for the NM (top), FM (middle), and AF (bottom) configurations.

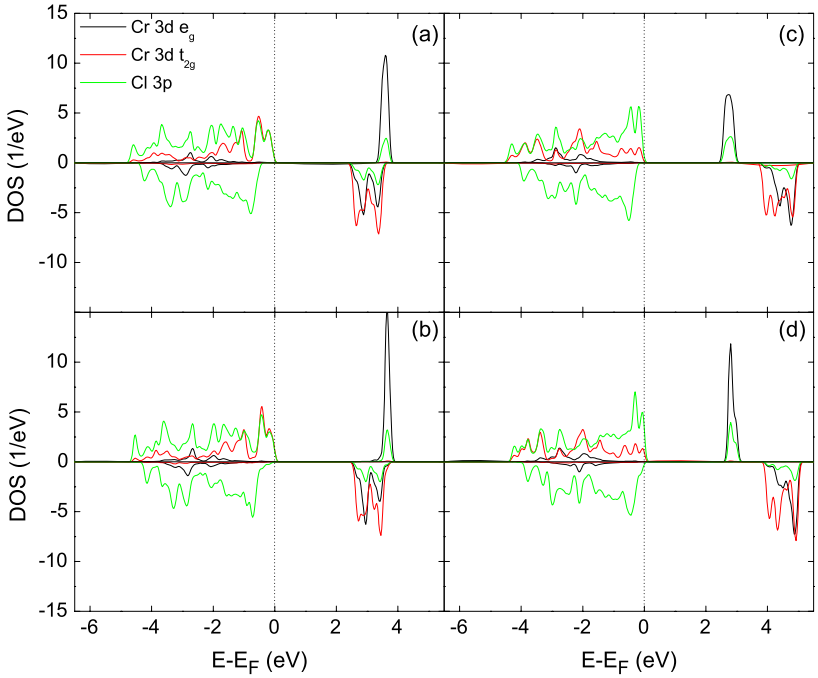

Figure 5. Partial DOS of monoclinic $CrCl_3$ obtained from GGA + AMF (left) and GGA + HMF (right) calculations for the FM (top) and AF (bottom) configurations.

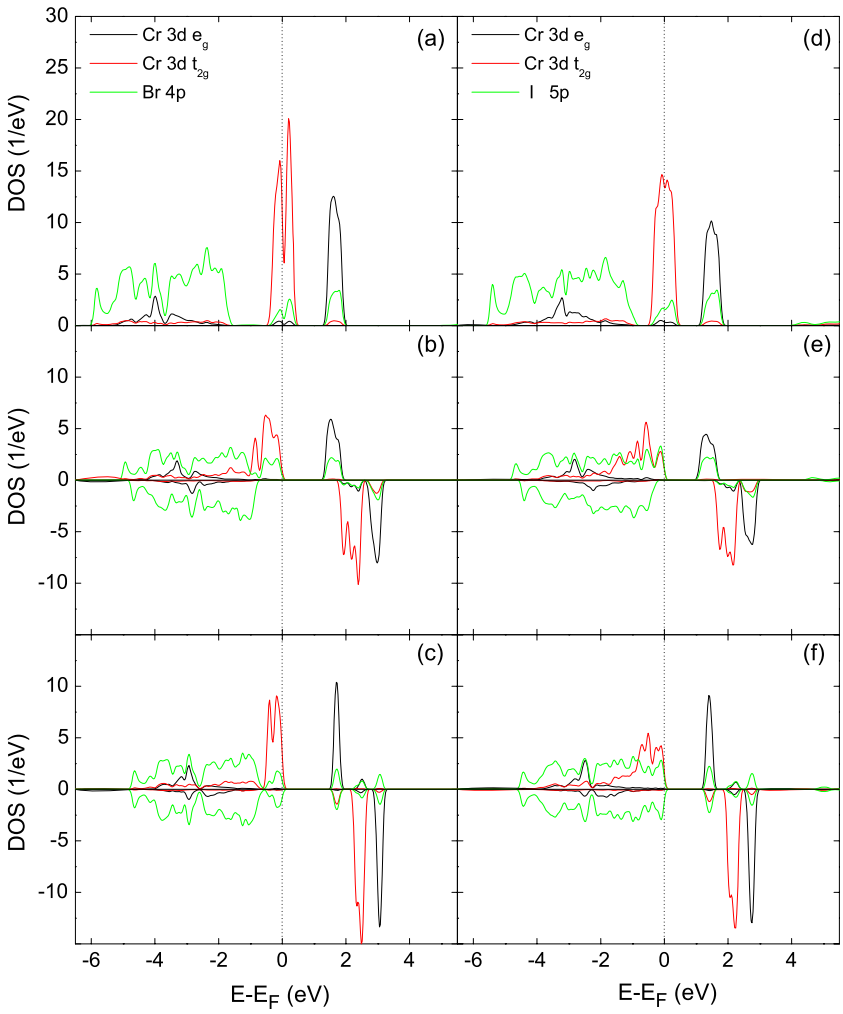

Figure 6. Partial DOS of trigonal $CrBr_3$ (left) and CrI_3 (right) obtained from GGA calculations for the NM (top), FM (middle), and AF (bottom) configurations.

unphysical in this case the NM calculations did not converge and no respective data could be derived. It turns out that the FM and AF total energies are almost degenerate for all GGA + U methods. Resembling the findings in the trigonal case, the results of the GGA + HMF and GGA + AMF methods are distinguished by the energetical order of the unoccupied spin majority and minority states.

In order to study the AF ordering of $CrCl_3$, we compare the total energies of the two possible structures of this compound for the different band structure methods and magnetic configurations. For the GGA method, we find the lowest energy for the trigonal structure combined with FM ordering. It is 9.5 meV lower than the second lowest configuration, which is the monoclinic structure combined with AF ordering. For both the GGA + HMF and GGA + SIC methods, the same energetical order is realized, with the FM trigonal configuration 9.3 meV and 9.1 meV, respectively, below the AF monoclinic configuration. Only the GGA + AMF method yields the AF ground state which is clearly indicated by experiments. Therefore, we will subsequently focus on this approach.

For the trigonal structure the AF ordered configuration is 10.0 meV favoured against the FM configuration, while for the monoclinic structure this energy difference is only 1.7 meV. That means a structural phase transition from monoclinic to trigonal strongly supports AF ordering with respect to FM ordering. Moreover, comparing the two AF ordered cases to each other, the calculation for the trigonal structure results in an total energy which is 17.1 meV below that of the monoclinic structure. Therefore, our results strongly indicate that the crystal structure of $CrCl_3$ at low temperature is rather trigonal than monoclinic and that this symmetry breaking supports the AF ordering.

On going from the monoclinic to the trigonal structure, i.e. from a face-centred cubic closed-packed to a hexagonal arrangement of the halide atoms, neighbouring halide–Cr–halide triple layers are shifted perpendicular to the hexagonal c-axis. This modifies the Cl–Cl orbital overlap connecting them and thus the interlayer magnetic exchange. However, note that our calculations give no hint at the true structure of $CrCl_3$. We have used the monoclinic structure reported by Morosin and Narath as a reference in order to judge whether a lowering of the symmetry to $R\bar{3}$ would enhance the AF instability. In contrast to the model calculations of Feldkemper and Weber [18] for a Mott–Hubbard insulator, our electronic structure calculations indicate that the $R\bar{3}$ structure

has a lower energy than the $C2/m$ structure. Yet, there could exist another configuration which might have an even lower energy. To finally resolve the low temperature crystal structure of $CrCl_3$ new x-ray diffraction or neutron experiments would be required.

We observe increasing Cr–halide bond lengths on going from the chloride to the iodide, see table 1. In general, longer bond lengths result in smaller band widths of the partially occupied t_{2g} states. The increased DOS at the Fermi level enhances the magnetic instability. $CrBr_3$ and CrI_3 thus order ferromagnetically, as is reflected by the energy differences summarized in table 4. Figure 6 comprises the electronic structure results for $CrBr_3$ (left) and CrI_3 (right). The band structures of the two compounds are similar to that of $CrCl_3$ and therefore are not shown. As they have trigonal symmetry, it is not surprising that our calculations result in FM ordering rather than AF ordering, see table 4, which perfectly agrees with experimental results [5]. The moment is larger for CrI_3 than for $CrBr_3$, whereas the insulating energy gap is larger for $CrBr_3$. The t_{2g}–e_g splitting due to the octahedral coordination of the Cr sites strongly decreases from the chloride to the bromide and iodide. This confirms the trend of increasing bond lengths and enhancement of the magnetic instability.

The calculated Cr–Br hybridization amounts to about 10%, confirming the estimates of Carricaburu *et al* [15] from valence band photoemission spectroscopy. Our calculations yield a Cr moment of 2.84 μ_B for ferromagnetic $CrBr_3$, which is very close to the moment of 2.83 μ_B found in the neutron-diffraction study of Radhakrishna and Brown [20]. Due to the well-known shortcomings of the GGA, the calculated energy gap of 1.37 eV is smaller than the experimental gap of 2.1 eV resulting from the photoconductivity spectra of Kanazawa and Street [28].

4. Conclusion

The electronic and magnetic properties of the isostructural chromium halides $CrCl_3$, $CrBr_3$, and CrI_3 have been investigated in detail by means of density functional theory. The electronic structure of the compounds are dominated by the Cr 3d states at the Fermi level. More specifically, the magnetic ordering is governed by a complex interplay between FM and AF instabilities within and perpendicular to the characteristic halide–Cr–halide triple layers. Due to increasing Cr–halide bond lengths (within the Cr–halide octahedra) the FM instability inherent to all three systems becomes stronger along the series chloride, bromide, and iodide. For $CrCl_3$ a symmetry breaking distortion of the crystal structure, accompanied by AF ordering along the hexagonal c-axis, in fact is favourable according to experimental results.

However, our calculations indicate that the AF ground states cannot be reproduced by the GGA, GGA + HMF, and GGA + SIC electronic structure methods, while the GGA + AMF approach gives results which are in agreement with the experimental situation. Total energies obtained by the GGA + AMF approach for fully optimized crystal structures show that a transition from a monoclinic to a trigonal symmetry results in an energy gain of 17.1 meV per (trigonal) unit cell. Therefore our calculations strongly support the original claim of Morosin and Narath [19] of a low temperature phase transition in $CrCl_3$. However, because the proposed $R\bar{3}$ symmetry has been excluded by Feldkemper and Weber [18], an experimental reinvestigation of the low temperature crystal structure of $CrCl_3$ would be desirable.

References

[1] Goodenough J B 1955 *Phys. Rev.* **100** 564
[2] Kanamori J 1959 *J. Phys. Chem. Solids* **10** 87
[3] Anderson P W 1959 *Phys. Rev.* **115** 2
[4] Tsubokawa I 1960 *J. Phys. Soc. Japan* **15** 1664
[5] Bené R W 1969 *Phys. Rev.* **178** 497
[6] Starr C, Bitter F and Kaufmann A R 1940 *Phys. Rev.* **58** 977
[7] de Jongh L J and Miedema A R 1974 *Adv. Phys.* **23** 1
[8] Samuelsen E J, Silberglitt R, Shirane G and Remeika J P 1971 *Phys. Rev.* B **3** 57
[9] Alyoshin V A, Berezin V A and Tulin V A 1997 *Phys. Rev.* B **56** 719
[10] Davis H L and Narath A 1964 *Phys. Rev.* **134** A433
[11] Narath A and Davis H L 1965 *Phys. Rev.* **137** A163
[12] Pollini I 1994 *Phys. Rev.* B **50** 2095
[13] Pollini I 1999 *Phys. Rev.* B **60** 16170
[14] Pollini I 2003 *Phys. Rev.* B **67** 155111
[15] Carricaburu B, Mamy R and Pollini I 1991 *J. Phys.: Condens. Matter* **3** 8511
[16] Antoci S and Mihich L 1978 *Phys. Rev.* B **18** 5768
[17] Shinagawa K, Sato H, Ross H J, McAven L F and Butler P H 1996 *J. Phys.: Condens. Matter* **8** 8457
[18] Feldkemper S and Weber E 1998 *Phys. Rev.* B **57** 7755
[19] Morosin B and Narath A 1964 *J. Chem. Phys.* **40** 1958
[20] Radhakrishna P and Brown P J 1987 *Phys. Rev.* B **36** 8765
[21] Schwingenschlögl U, Eyert V and Eckern U 2003 *Europhys. Lett.* **61** 361
Schwingenschlögl U, Eyert V and Eckern U 2003 *Europhys. Lett.* **64** 682
[22] Eyert V, Schwingenschlögl U and Eckern U 2004 *Chem. Phys. Lett.* **390** 151
Eyert V, Schwingenschlögl U and Eckern U 2005 *Europhys. Lett.* **70** 782
[23] Blaha P, Schwarz K, Madsen G K H, Kvasnicka D and Luitz J 2001 *Wien2k. An Augmented Plane Wave + Local Orbitals Program for Calculating Crystal Properties* TU Vienna
[24] Schwingenschlögl U and Schuster C 2007 *Phys. Rev. Lett.* **99** 237206
Schwingenschlögl U and Schuster C 2007 *Euro. Phys. Lett.* **79** 27003
[25] Czyzyk M T and Sawatzky G A 1994 *Phys. Rev.* B **49** 14211
[26] Anisimov V I, Zaanen J and Andersen O K 1991 *Phys. Rev.* B **44** 943
[27] Anisimov V I, Solvoyev I V, Korotin M A, Czyzyk M T and Sawatzky G A 1993 *Phys. Rev.* B **48** 16929
[28] Kanazawa K K and Street G B 1970 *Phys. Status Solidi* b **38** 445